Plasmonic pressure sensor based on Fano resonance assisted by photo-elastic material

R. YU, F. CHEN*, S. WU, R. BI
School of Physics and Optoelectronic Engineering, Yangtze University, Jingzhou, 434023, China
Institute of Quantum Optics and Information Photonics, Yangtze University, Jingzhou 434023, China

In this work, the pressure control of Fano resonance is presented, the proposed structure is composed of a MIM (metal-insulator-metal) waveguide side coupled to a rectangle resonator, and the rectangle resonator is filled with photo-elastic material which can tune the Fano resonance by pressure. The transmittance and sensing performance is calculated by two-dimensional finite difference time domain method. The Fano resonance is originated from the coupling between the ultra-narrow discrete states and the broad continua state. In the proposed system, the discrete state is from the side coupled rectangle resonator and the continua state is from the stub resonator. The asymmetrical Fano linestyle can be tuned by changing the pressure to the silicon or the structure parameters. The sharp transmission spectrum contributes to a high efficient plasmonic pressure sensor, which can yield a linear sensitivity of 15 nm/GPa. The proposed plasmonic structure may have application in the slow light device, nanoscale filter, all-optical switch and pressure sensor.

(Received July 12, 2019; accepted February 17, 2020)

Keywords: Surface plasmon polariton, Rectangle resonator, Fano resonance, Pressure sensing

1. Introduction

Surface plasmon polaritons (SPPs) have the ability to control the light on subwavelength and overcome the classical diffraction limit [1-3]. Surface plasmons are considered to have application in the design of highly integrated optical circuits over recent years. Many plasmonic structures based on SPPs have been investigated both numerically and experimentally. Such as wavelength demultiplexers [4], plasmonic sensor [5-6], band-stop and band-pass filter [7-9], optical switching [10], slow light [11-13], logic gates and Mach-Zehnder interferometers [14-15]. Plasmonic sensors based on Fano resonance have been realized in many structures. For example, MIM stub waveguide coupled-resonator [16], MIM waveguide with oblique rectangular cavity [17], rod and concentric square ring disk nanostructure [18]. MIM waveguide coupled-resonator systems are widely used in nanophotonics since it has great advantages in refractive index sensing and optical switch. In addition, MIM waveguide is suitable for integration due to its capability of overcoming the diffraction limit. There are many optical sensors have been designed for sensing the various variables, such as refractive index, temperature, pressure, current, voltage, and force. For example, Li et al. investigated the transient and tunable plasmonic properties of Mg in the environmental and biomedical sensor [19]. Lou et al. proposed and investigated a plasmonic multifunction temperature sensor with high sensitivity in waveguide structure [20]. Huang er al. Proposed a refractive index sensor based on plasmon-induced transparency in side coupled stub hexagon resonators [21]. For dynamically tunable Fano resonance the traditional method is directly adjusting geometrical parameters, but it is inconvenient to adjust the size when the device has been made. In our previous paper [22-25], graphene, Kerr material, liquid crystal material and optofluidic technology are utilized to design tunable all-optical switch, plasmonic filter, tunable plasmonic splitter, Fano resonance and sensor.

Motivated by the work [26-29], in this literature, a Fano resonance structure based on stub MIM waveguide side coupled rectangular resonator is proposed. The rectangular cavity is filled with photo-elastic material silicon. The Fano resonance and sensing performance are investigated by two-dimensional finite difference time domain method, the results show that the resonant wavelength, linewidth can also be tuned by the geometric parameters. Moreover, the comparison of the proposed pressure sensing with other work is displayed. Therefore, the proposed pressure plasmonic sensor may find potential application in automobile industries, avionics system, biomedicine and petrochemical industry hazard control [30-32].

2. Geometry and simulation method

Fig. 1 shows the proposed plasmonic waveguide coupled resonator system which is composed of a MIM waveguide with stub resonator and a rectangle resonator. In the simulation, a two dimensional (xy plane) model is used. The metal in the model is silver, and the frequency-dependent complex relative permittivity of silver is characterized by the Drude model:

$$\varepsilon(\omega) = 3.7 - \frac{\omega_p^2}{(\omega^2 + i\omega\gamma_p)} \tag{1}$$

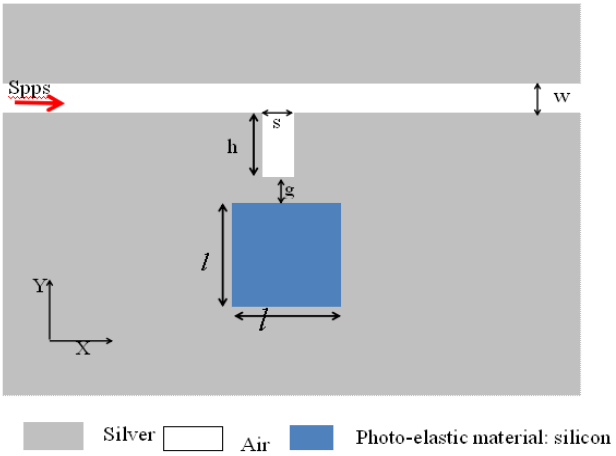

Fig. 1. The schematic diagram of the proposed plasmonic sensor composed of a rectangle resonator filled with photo-elastic material: silicon and a stub MIM waveguide. The geometrical parameters were set as $w = 50\,nm$, $h = 210\,nm$, $s = 60\,nm$, $l = 120\,nm$, $g = 10\,nm$

where the plasma frequency of silver $\omega_p = 9.1ev$, and the damping constant γ=0.018ev [33]. The insulator in the MIM waveguide is air. The width of the bus waveguide is denoted by w, the length and width of the stub resonator are denoted by h and s. The side length of the rectangle cavity is l. The gap between the stub and the rectangle cavity is g. The rectangular cavity is filled with photonic-elastic material silicon, whose refractive index can be calculated by:

$$n = n_0 - (\alpha + 2\beta)\sigma \tag{2}$$

the parameters α and β are defined as follows:

$$\alpha = \frac{n_0^3(p_{11} - 2Vp_{12})}{2E}, \beta = \frac{n_0^3[p_{12} - V(p_{11} + p_{12})]}{2E} \tag{3}$$

where σ is the applied hydrostatic pressure, n_0 is the refractive index of the silicon at zero pressure, V is the Poisson ratio, P_{ij} is the stress-optic constant and E is the Young modulus. The refractive index of the silicon increases 0.0385 while increasing the applied pressure by $1GPa$ [34-35]. Perfect matched layers (PMLs) and metal boundary condition are applied in X and Y direction. The grid sizes are set to be $\Delta x = \Delta y = 3\,nm$, $\Delta t = \frac{\Delta x}{2c}$, where c is the free- space speed of light. The total simulation area is $1400\,nm \times 1400\,nm$. In this paper, the performance of the proposed Fano resonance has been simulated by 2D FDTD method with matlab 7.0 software, more accurate results can be obtained by 3D FDTD method but at the cost of a larger number of computer memory and time.

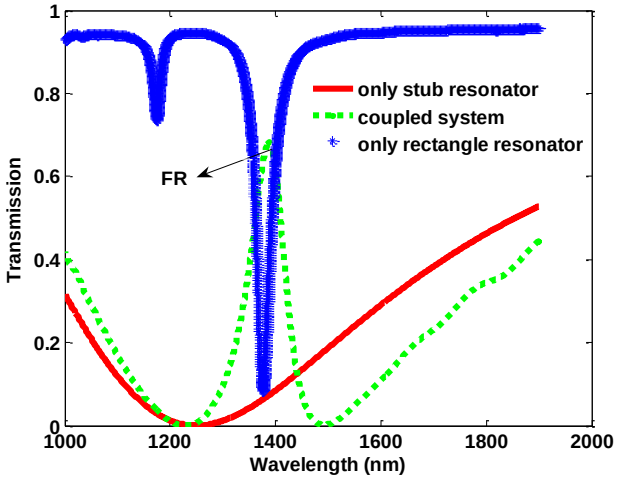

Fig. 2. The FDTD simulation results. The transmission spectra of the single stub resonator, single rectangle resonator, and coupled plasmonic system without applied- pressure

3. Simulation results and discussions

In the simulation, the geometric parameters of the proposed structure are set as: $w = 50\,nm$, $h = 210\,nm$, $s = 60\,nm$, $l = 120\,nm$, $g = 10\,nm$. In the proposed plasmonic structure, the stub resonator can be directly excited by the input SPPs while the rectangular cavity can only be coupled to the stub resonator. Therefore the rectangular cavity and the stub resonator are regarded as dark mode resonator and bright mode resonator, respectively. The transmission spectra of the MIM

waveguide with stub resonator, single rectangular cavity and the whole Fano coupled system are presented in Fig 2. The red line stands for the transmission which only a MIM waveguide with a stub resonator, it can be observed that the spectrum is very broad which can be seen as a continuum state. To create a discrete state, a rectangular cavity is side coupled to stub waveguide, noted that at 1375 nm, there is a narrow Lorentzian like valley which represents the $TM_{1,0}$ eigen mode of the rectangular cavity. Since the narrow resonant mode is overlapped with the broad continuum state. Therefore, sharp and asymmetric Fano resonances are formed. The transmittance is about 68% at the peak wavelength of 1389 nm, and the transmittance is zero at 1492 nm. It is believed that the sharp Fano resonance can be used to design slow light or refractive index sensors.

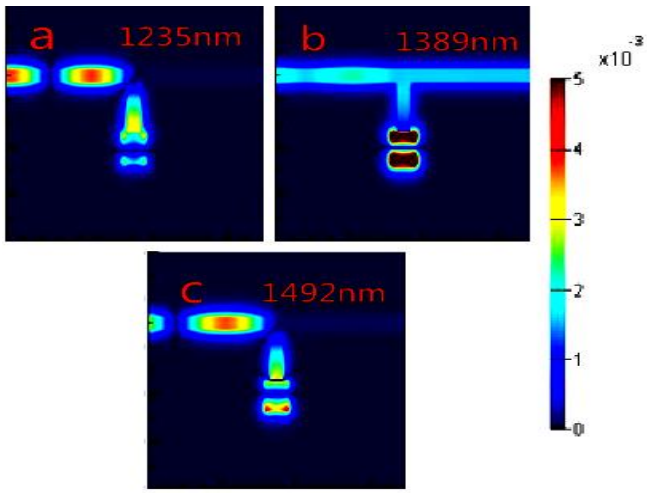

Fig. 3. Magnetic field distributions at the wavelength 1235 nm (a), 1389 nm (b), 1492 nm (c), respectively (color online)

To further understand the physical mechanism of the Fano resonance, the magnetic field-distributions $|H_z|$ at the wavelength of the transmission peak (1389 nm) and two transmission dips (1235 nm, 1492 nm) are demonstrated in Fig. 3. For comparison, all the field distribution Figs are normalized, and the color bar values are identical. It can be observed from Fig. 3a and 3c that the $|H_z|$ between the waveguide and the stub resonator are always out of phase and no SPPs can pass through the bus waveguide. The profile of $|H_z|$ at the peak wavelength is displayed in Fig. 3 b. It can see that the dark mode resonator is strongly excited and a part of input SPPs can pass through the waveguide. The high on-off contrast ratio of the proposed Fano resonance can be achieved, which has potential application in ultrafast optical switches or sensors.

Next, the impact of the structure parameters on the transmission performance is investigated. The effect of gap distance g on the transmission spectra is studied. Here, the other geometric parameters are the same as above, when gap distance $g=10, 20, 30\ nm$, the transmission spectrum is displayed in Fig 4. It can see that when the gap distance g increases, the transmittance becomes smaller, and at the same time the linewidth becomes also smaller. Therefore, the high contrast ratio and narrow linewidth can be tuned by changing the gap distance g. As the discrete state is induced by the rectangular resonator. The effect of the side length of rectangular resonator on the transmission spectra is investigated, from Fig. 5 it can be observed that the Fano peak wavelength increases from 1386 nm to 1587 nm when the side length of the rectangular resonator increases from 120 nm to 160 nm. At the same time, the symmetric Lorentzian line shape changes gradually to asymmetric Fano line shape with a side length of 160 nm. The results indicate that the Fano line shape is determined by the resonant wavelength difference between the stub resonator and the rectangular cavity.

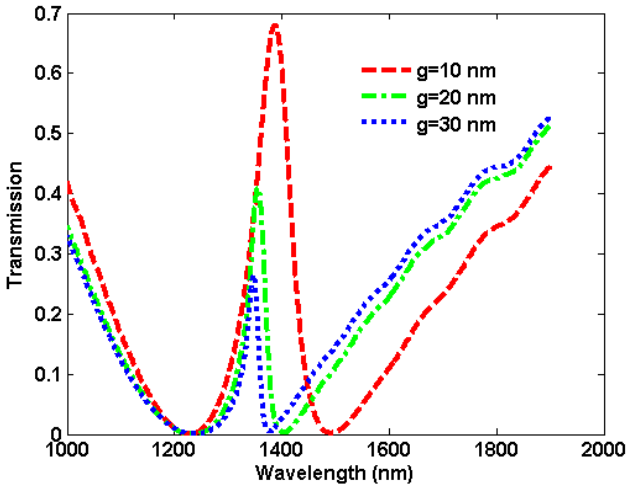

Fig. 4. The transmission spectra of the plasmonic sensor system with a different gap g (color online)

In the proposed Fano resonance, the continua state is induced by the stub resonator, the effect of the stub size on the transmission spectra is calculated. From Fig. 6, it can be noticed that when the length of the stub resonator decrease, the symmetric Lorentzian line shape changes gradually to asymmetric Fano line shape, but the resonant peak wavelengths remain unchanged. Similar to the rectangular resonator size regulation, the resonant wavelength difference between the stub and the

rectangular cavity can also be changed by varying stub size. Therefore, the proposed plasmonic waveguide structure can be used as a pressure sensor.

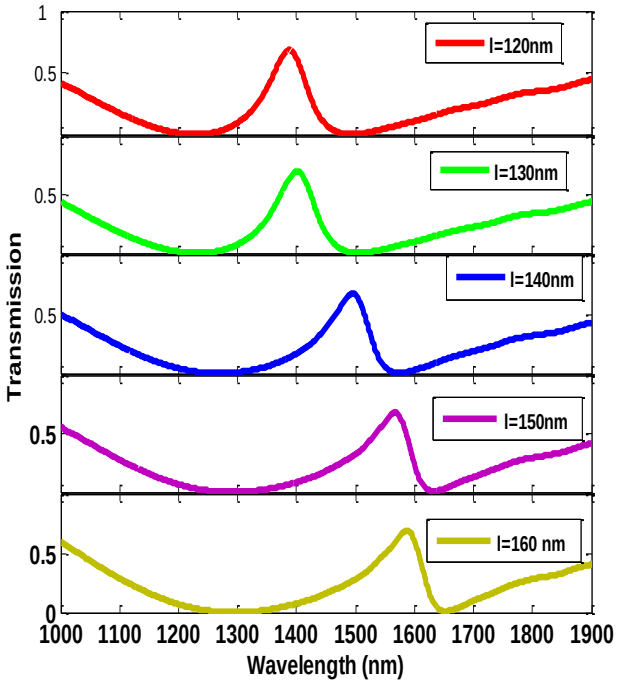

Fig. 5. The transmission spectra of the plasmonic sensor system with different side lengths l of rectangle resonator

The refractive index of the photo-elastic material silicon can be tuned by the pressure. Therefore the Fano resonance peaks can be tuned by the pressure. Fig. 7(a) shows the transmission spectra of the plasmonic Fano system with different pressures to the rectangular cavity. According to our simulations, as the pressure increases, the Fano resonant wavelength is red shifted. In the absence of the pressure, the resonant wavelength is 1388 nm, while when the applied pressure is 6 GPa, the resonant wavelength moves to 1480 nm. The time averaged magnetic-field (1449 nm) intensity distributions are presented in Fig. 7 (b)-(e). By increasing the pressure, the refractive index n of the silicon increase as well, the optical length of the rectangular resonator increase. There, the resonant frequency will be varied with the pressure. Therefore, the proposed plasmonic waveguide structure can be used as a pressure sensor.

The pressure effect on the proposed plasmonic Fano structure is analyzed by increasing the pressure from 0 to 6GPa. In the pressure sensor simulation, geometrical parameters are set to be: $w = 50\,nm$, $h = 210\,nm$, $s = 60\,nm$, $l = 120\,nm$, $g = 10\,nm$. Fig. 8 shows the relationship between the pressure and the resonant wavelengths. It can be seen that the resonant wavelength varies linearly with the pressure, the regression coefficient R^2 is calculated and its value is 0.982. To better evaluate the pressure sensing performance, the pressure sensitivity (S_p) is defined as the ratio of change in the resonant wavelength due to the applied pressure variation.

$$S_P = \frac{\Delta\lambda}{\Delta P} \tag{4}$$

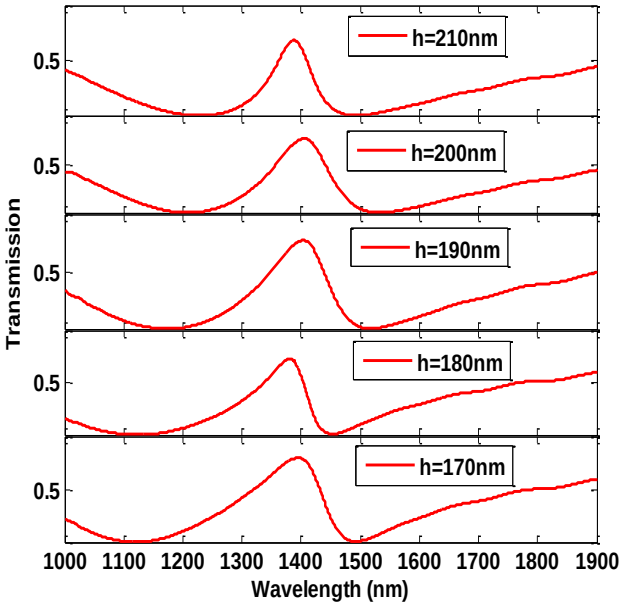

Fig. 6. The transmission spectra of the plasmonic Fano system with different lengths of stub resonator h

where $\Delta\lambda$ and Δp are the resonant wavelength shift and pressure difference, respectively. For the proposed plasmonic structure the pressure sensitivity (S_P) is calculated as $15nm/GPa$, the result is bigger than the hexagonal photonic crystal ring resonator structure reported in the paper [36]. For sensing applications, a high-quality factor ($Q = \frac{\lambda}{\Delta\lambda}$) is desired, here λ is the resonance wavelength and $\Delta\lambda$ stands for the wavelength difference at FWHM. The quality factor of the present structure is also calculated and the results of is 15.9. The pressure sensor functional parameters are compared with the previous sensors which are listed in Table 1. From Table 1, it can be deduced that our proposed plasmonic pressure sensor possesses a higher pressure sensitivity bu at the cost of quality factor.

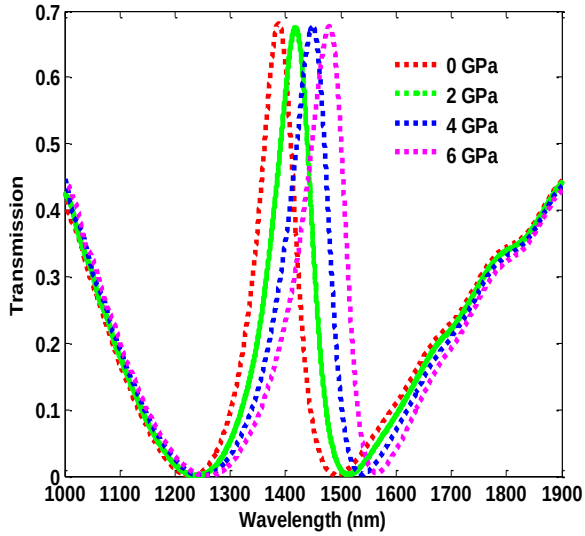

(a)

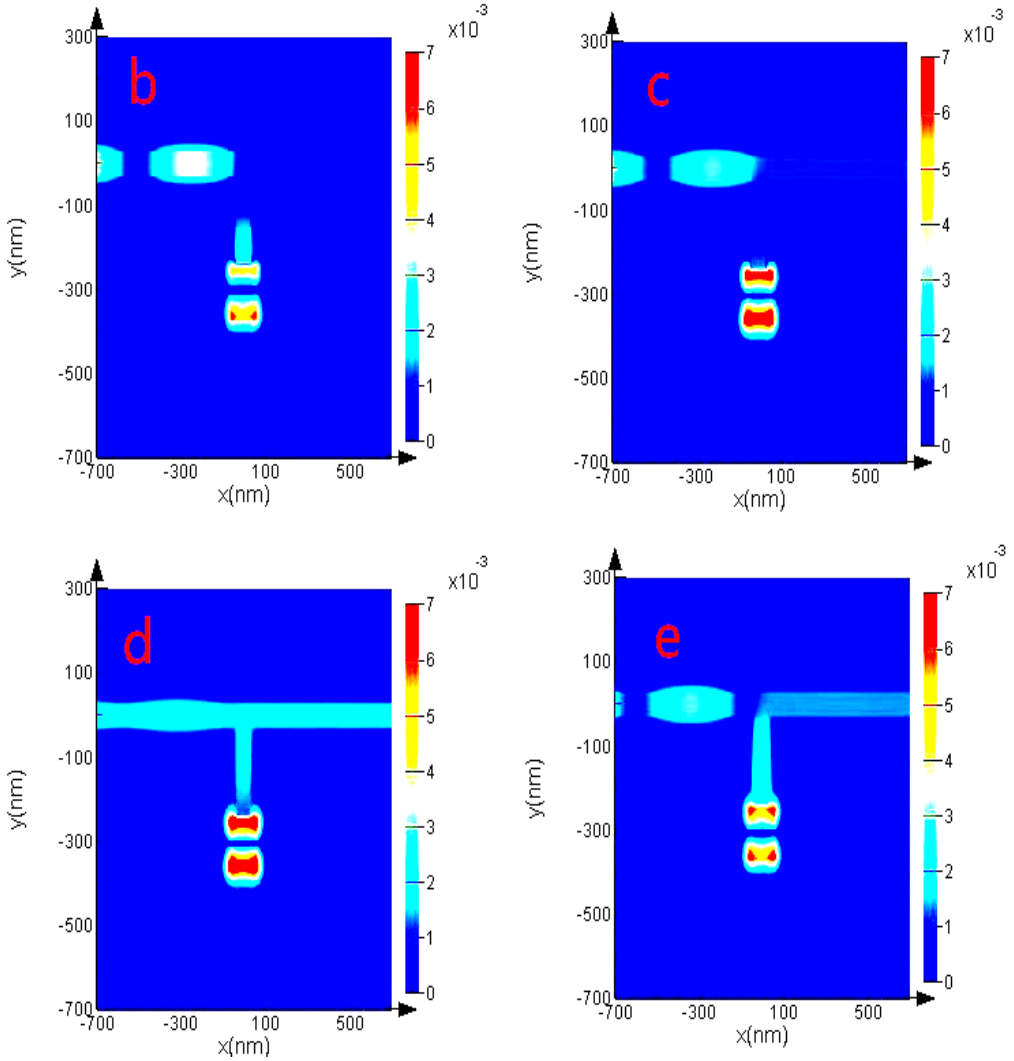

Fig. 7. (a) The transmission spectra of the plasmonic Fano system with different pressures to silicon filled in the rectangle resonator. FDTD simulations of the time averaged magnetic field ($\lambda = 1449nm$) intensity distribution when (b) 0 Gpa *(c)* 2 Gpa *(d)* 4 Gpa *(e)* 6 Gpa *(color online)*

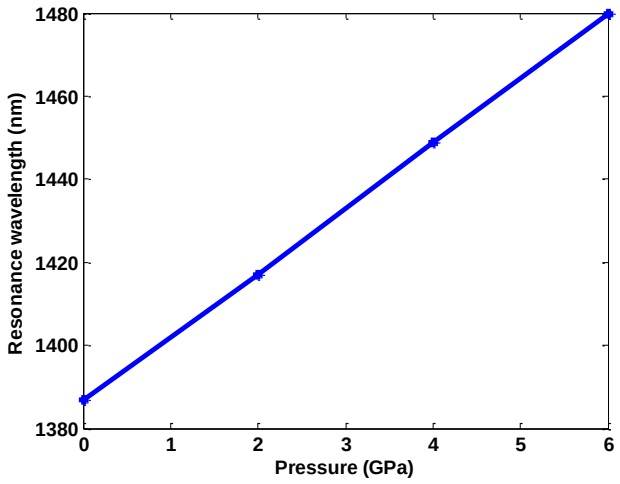

Fig. 8. A linear relationship between pressure and the resonant wavelengths of the Fano effect

Table 1. Comparison of the proposed pressure sensing performance with other works

Reference	Pressure range (GPa)	Transmission Efficiency (%)	Sensitivity (nm/GPa)	Quality factor
This work	0-6	68	15	15.9
R 36	0.05-6	100	9.66	749
R 34	0-7	57.5	2	75.5
R 37	0-4	60	1.5	150

4. Conclusion

In this paper, the Fano sharp line shape has been investigated numerically in plasmonic waveguide systems which consist of a stub resonator and rectangular cavity. Embedding photo-elastic material silicon in the rectangular cavity has been used to modulate the Fano resonance. Numerical calculation results indicate that the Fano resonant wavelength, line shape can be tuned by the geometric parameters. Such as the length of the stub resonator, the side length of the rectangular cavity, the gap distance of the stub resonator and rectangular cavity. Moreover, the Fano resonance can also be tuned by the pressure. The pressure sensitivity and the quality factor of the proposed structure are 15 nm/ GPa and 15.9. The pressure sensitivity is excellent compared with the other works. The above results can find potential applications in highly integrated circuits, plasmonic nanosensor and industrial safety.

Acknowledgements

This work is supported by the Yangtze Youth Fund (Grant No. 2016cqn55), Yangtze Fund for Youth Teams of Science and Technology Innovation (Grant No. 2015cqt03). National Natural Science Foundation of China (Grant No. 11747091).

References

[1] K. F. MacDonal, N. I. Zheludev, Laser Photonics Rev. **4**(4), 562 (2010).
[2] W. L. Barnes, A. Dereux, T. W. Ebbesen, Nature **424**(6950), 824 (2003).
[3] M. A. Butt, S. N. Khonina, N. L. Kazanskiy, Laser Physics Letters **16**(12), 126201 (2019).
[4] Z. Chen, R. Hu, L. N. Cui, L. Yu, L. L. Wang, J. H. Xiao, Optics Communications **320**, 6 (2014).
[5] H. Lu, X. M. Liu, D. Mao, G. X. Wang, Opt. Lett. **37**(18), 3780 (2012).
[6] N. L. Kazanskiy, S. N. Khonina, M. A. Butt, Physica E **S1386-9477**(19), 31133 (2019).
[7] H. Lu, X. M. Liu, Y. K. Gong, L. R. Wang, D. Mao, Optics Communications **284**, 2613 (2011).
[8] T. Xu, Y. K. Wu, X. G. Luo, L. J. Guo, Nature Communications **1**(59), 1 (2010).
[9] X. S. Lin, X. G. Huang, Opt. Lett. **33**(23), 2874 (2008).
[10] D. M. Beggs, T. P. White, L. O. Faolain, T. F. Krauss, Opt. Lett. **33**(2), 147 (2008).
[11] C. Wu, A. B. Khanikaev, G. Shvets, Phys. Rev. Lett. **106**(10), 107403 (2011).
[12] K. Totsuka, N. Kobayashi, M. Tomita, Phys. Rev. Lett. **98**(21), 213904 (2007).
[13] G. Lai, R. S. Liang, Y. J. Zhang, Z. Y. Bian, L. X. Yi, G. Z. M. Zhan, R. T. Zhao, Opt. Express **23**(5), 6554 (2015).
[14] M. Pu, N. Yao, C. Hu, X. Xin, Z. Zhao, C. Wang, X. Luo, Opt. Express **18**(20), 21031 (2010).
[15] Y. Bian, Q. Gong, Optics Communications **313**, 27 (2014).
[16] B. F. Yun, R. H. Zhang, G. H. Hu, Y. P. Cui, Plasmonics **11**(4), 1157 (2016).
[17] S. F. Pang, Y. P. Huo, Y. Xie, L. M. Hao, Optics Communications **381**, 409 (2016).
[18] Y. Y. Huo, T. Q. Jia, Y. Z. Zhang, H. Zhao, S. A. Zhang, D. H. Feng, Z. R. Sun, Sensors **13**, 11350 (2013).
[19] R. M. Li, S. X. Xie, L. B. Zhang, L. Q. Li, D. Y. Kong, Q. Wang, R. Xin, X. Sheng, L. Yin, C. J. Yu, Z. F. Yu, X. R. Wang, L. Gao, Nano Res. **11**, 4390 (2018).
[20] J. Zhu, J. Lou, Molecules **23**, 2700 (2018).
[21] C. Wu, H. F. Ding, T. Y. Huang, X. Wu, B. W. Chen, K. X. Ren, S. N. Fu, Plasmonics **13**(1), 251 (2018).

[22] F. Chen, J. Mod. Opt. **64**(15), 1531 (2017).
[23] F. Chen, D. Z. Yao, Y. N. Liu, Appl. Phys. Express **7**, 082202 (2014).
[24] F. Chen, D. Z. Yao, J. Mod. Opt. **61**(18), 1486 (2014).
[25] F. Chen, D. Z. Yao, Optics Communications **312**, 143 (2013).
[26] G. Y. Duan, P. L. Lang, L. L. Wang, L. Yu, X. H. Xiao, Mod. Phys. Lett. B **30**(21), 1650284 (2016).
[27] P. Palizvan, S. Olyaee, M. Seifouri, Journal of Nanoelectronics and Optoelectronics **13**(10), 1449 (2018).
[28] P. Palizvan, S. Olyaee, M. Seifouri, Photonic Sensors **8**(3), 242 (2018).
[29] S. Olyaee, A. A. Dehghani, Sensor Letters **11**(10), 1854 (2013).
[30] H. Xu, M. Hafezi, J. Fan, J. M. Taylor, G. F. Strouse, Z. Ahmed, Opt. Express **22**(3), 3098 (2014).
[31] Y. Zhang, J. Huang, X. Lan, H. Xiao, Opt Engineering **53**(6), 067101 (2014).
[32] P. Palizvan, S. Olyaee, M. Seifouri, Photon. Sens. **8**(3), 242 (2018).
[33] H. Lu, X. M. Liu, D. Mao, Y. K. Gong, G. X.Wang, Opt. Lett. **36**(16), 3233 (2011).
[34] K.V. Shanthi, S. Robinson, Photon. Sens. **4**(3), 248 (2014).
[35] M. Huang, Int. J. Solids Struct. **40**, 1615 (2003).
[36] R. Rajasekar, S. Robinson, Plasmonics **14**, 3 (2019).
[37] T. Dharchana, A. Sivanantharaja, S. Selvedran, Adv. Nat. App. Sci. **11**, 26 (2017).

*Corresponding author: chenfang@yangtzeu.edu.cn